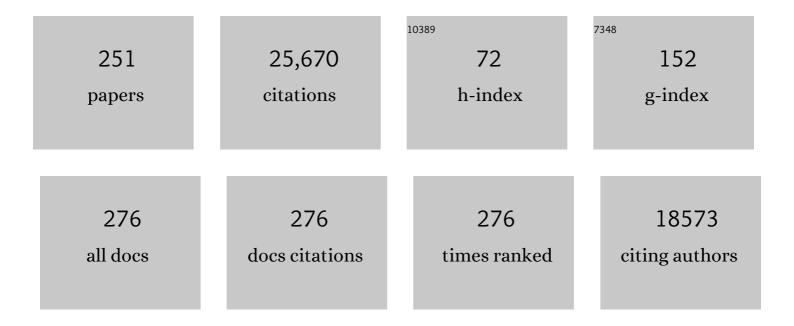
Ravi S Menon

List of Publications by Year in descending order

Source: https://exaly.com/author-pdf/6183662/publications.pdf Version: 2024-02-01



#	Article	IF	CITATIONS
1	Functional Organization of Frontoparietal Cortex in the Marmoset Investigated with Awake Resting-State fMRI. Cerebral Cortex, 2022, 32, 1965-1977.	2.9	1
2	Toward next-generation primate neuroscience: A collaboration-based strategic plan for integrative neuroimaging. Neuron, 2022, 110, 16-20.	8.1	22
3	An open access resource for functional brain connectivity from fully awake marmosets. NeuroImage, 2022, 252, 119030.	4.2	23
4	Integration of an RF coil and commercial field camera for ultrahighâ€field MRI. Magnetic Resonance in Medicine, 2022, 87, 2551-2565.	3.0	5
5	Effects of MP2RAGE B1+ sensitivity on inter-site T1 reproducibility and hippocampal morphometry at 7T. NeuroImage, 2021, 224, 117373.	4.2	17
6	Radiofrequency coil for routine ultraâ€highâ€field imaging with an unobstructed visual field. NMR in Biomedicine, 2021, 34, e4457.	2.8	18
7	Schrödinger filtering: a precise EEG despiking technique for EEG-fMRI gradient artifact. NeuroImage, 2021, 226, 117525.	4.2	8
8	Normative Analysis of Individual Brain Differences Based on a Population MRI-Based Atlas of Cynomolgus Macaques. Cerebral Cortex, 2021, 31, 341-355.	2.9	12
9	Effects of phase regression on high-resolution functional MRI of the primary visual cortex. NeuroImage, 2021, 227, 117631.	4.2	15
10	Neural network of social interaction observation in marmosets. ELife, 2021, 10, .	6.0	22
11	Repetitive mild traumatic brain injury in mice triggers a slowly developing cascade of long-term and persistent behavioral deficits and pathological changes. Acta Neuropathologica Communications, 2021, 9, 60.	5.2	31
12	Muting, not fragmentation, of functional brain networks under general anesthesia. NeuroImage, 2021, 231, 117830.	4.2	14
13	Structural alterations in cortical and thalamocortical white matter tracts after recovery from prefrontal cortex lesions in macaques. Neurolmage, 2021, 232, 117919.	4.2	2
14	Automatic determination of the regularization weighting for waveletâ€based compressed sensing MRI reconstructions. Magnetic Resonance in Medicine, 2021, 86, 1403-1419.	3.0	14
15	Author Response: Longitudinal Changes of Brain Microstructure and Function in Nonconcussed Female Rugby Players. Neurology, 2021, 96, 968.2-969.	1.1	0
16	Concussion Acutely Decreases Plasma Glycerophospholipids in Adolescent Male Athletes. Journal of Neurotrauma, 2021, 38, 1608-1614.	3.4	9
17	Mesoscale hierarchical organization of primary somatosensory cortex captured by resting-state-fMRI in humans. NeuroImage, 2021, 235, 118031.	4.2	14
18	Receiver phase alignment using fitted SVD derived sensitivities from routine prescans. PLoS ONE, 2021, 16, e0256700.	2.5	0

Ravi S Menon

#	Article	IF	CITATIONS
19	Minimal specifications for non-human primate MRI: Challenges in standardizing and harmonizing data collection. NeuroImage, 2021, 236, 118082.	4.2	22
20	Interspecies activation correlations reveal functional correspondences between marmoset and human brain areas. Proceedings of the National Academy of Sciences of the United States of America, 2021, 118, .	7.1	26
21	Protocol-dependence of middle cerebral artery dilation to modest hypercapnia. Applied Physiology, Nutrition and Metabolism, 2021, 46, 1038-1046.	1.9	6
22	Simultaneous functional MRI of two awake marmosets. Nature Communications, 2021, 12, 6608.	12.8	15
23	Putative Concussion Biomarkers Identified in Adolescent Male Athletes Using Targeted Plasma Proteomics. Frontiers in Neurology, 2021, 12, 787480.	2.4	3
24	Comparison of resting-state functional connectivity in marmosets with tracer-based cellular connectivity. Neurolmage, 2020, 204, 116241.	4.2	50
25	Using variableâ€rate selective excitation (VERSE) radiofrequency pulses to reduce power deposition in pulsed arterial spin labeling sequence at 7 Tesla. Magnetic Resonance in Medicine, 2020, 83, 645-652.	3.0	5
26	Functional reorganization during the recovery of contralesional target selection deficits after prefrontal cortex lesions in macaque monkeys. NeuroImage, 2020, 207, 116339.	4.2	14
27	Direct visualization and characterization of the human zona incerta and surrounding structures. Human Brain Mapping, 2020, 41, 4500-4517.	3.6	21
28	Brain Metabolite Levels in Sedentary Women and Non-contact Athletes Differ From Contact Athletes. Frontiers in Human Neuroscience, 2020, 14, 593498.	2.0	5
29	Divergence of rodent and primate medial frontal cortex functional connectivity. Proceedings of the National Academy of Sciences of the United States of America, 2020, 117, 21681-21689.	7.1	76
30	Cortico-Subcortical Functional Connectivity Profiles of Resting-State Networks in Marmosets and Humans. Journal of Neuroscience, 2020, 40, 9236-9249.	3.6	25
31	Elimination of Iowâ€inversionâ€efficiency induced artifacts in wholeâ€brain MP2RACE using multiple RFâ€shim configurations at 7 T. NMR in Biomedicine, 2020, 33, e4387.	2.8	1
32	Dynamic Reconfiguration, Fragmentation, and Integration of Whole-Brain Modular Structure across Depths of Unconsciousness. Cerebral Cortex, 2020, 30, 5229-5241.	2.9	12
33	Looming and receding visual networks in awake marmosets investigated with fMRI. NeuroImage, 2020, 215, 116815.	4.2	26
34	Longitudinal changes of brain microstructure and function in nonconcussed female rugby players. Neurology, 2020, 95, e402-e412.	1.1	20
35	Altered Resting-State Functional Connectivity Between Awake and Isoflurane Anesthetized Marmosets. Cerebral Cortex, 2020, 30, 5943-5959.	2.9	36
36	Demonstration and suppression of respirationâ€related artifacts in Bloch–Siegert shiftâ€based B 1 + maps of the human brain. NMR in Biomedicine, 2020, 33, e4299.	2.8	1

#	Article	IF	CITATIONS
37	Accelerating the Evolution of Nonhuman Primate Neuroimaging. Neuron, 2020, 105, 600-603.	8.1	92
38	Face selective patches in marmoset frontal cortex. Nature Communications, 2020, 11, 4856.	12.8	34
39	Task-based fMRI of a free-viewing visuo-saccadic network in the marmoset monkey. NeuroImage, 2019, 202, 116147.	4.2	35
40	Resonate: Reflections and recommendations on implicit biases within the ISMRM. Journal of Magnetic Resonance Imaging, 2019, 49, 1509-1511.	3.4	1
41	Comparison of Multiple Sclerosis Cortical Lesion Types Detected by Multicontrast 3T and 7T MRI. American Journal of Neuroradiology, 2019, 40, 1162-1169.	2.4	34
42	Integrated radiofrequency array and animal holder design for minimizing head motion during awake marmoset functional magnetic resonance imaging. NeuroImage, 2019, 193, 126-138.	4.2	45
43	Shape Optimization of an Electric Dipole Array for 7 Tesla Neuroimaging. IEEE Transactions on Medical Imaging, 2019, 38, 2177-2187.	8.9	25
44	Exploring the limits of network topology estimation using diffusion-based tractography and tracer studies in the macaque cortex. Neurolmage, 2019, 191, 81-92.	4.2	28
45	Imaging outcome measures of neuroprotection and repair in MS. Neurology, 2019, 92, 519-533.	1.1	53
46	Linked MRI signatures of the brain's acute and persistent response to concussion in female varsity rugby players. NeuroImage: Clinical, 2019, 21, 101627.	2.7	19
47	Intrinsic functional clustering of anterior cingulate cortex in the common marmoset. NeuroImage, 2019, 186, 301-307.	4.2	25
48	Open-source hardware designs for MRI of mice, rats, and marmosets: Integrated animal holders and radiofrequency coils. Journal of Neuroscience Methods, 2019, 312, 65-72.	2.5	20
49	Intrinsic Functional Boundaries of Lateral Frontal Cortex in the Common Marmoset Monkey. Journal of Neuroscience, 2019, 39, 1020-1029.	3.6	26
50	Magnetic field probes for timeâ€domain monitoring of RF exposure within tissueâ€mimicking materials for MRIâ€compatible medical device testing. Electronics Letters, 2018, 54, 16-18.	1.0	12
51	Reduced brain glutamine in female varsity rugby athletes after concussion and in non oncussed athletes after a season of play. Human Brain Mapping, 2018, 39, 1489-1499.	3.6	24
52	Prediction of radiation necrosis in a rodent model using magnetic resonance imaging apparent transverse relaxation (\$R_{2}^{*}\$). Physics in Medicine and Biology, 2018, 63, 035010.	3.0	6
53	Higher order thalamic nuclei resting network connectivity in early schizophrenia and major depressive disorder. Psychiatry Research - Neuroimaging, 2018, 272, 7-16.	1.8	20
54	Apparent transverse relaxation () on <scp>MRI</scp> as a method to differentiate treatment effect (pseudoprogression) versus progressive disease in chemoradiation for malignant glioma. Journal of Medical Imaging and Radiation Oncology, 2018, 62, 224-231.	1.8	5

#	Article	IF	CITATIONS
55	An Open Resource for Non-human Primate Imaging. Neuron, 2018, 100, 61-74.e2.	8.1	190
56	Concentric radiofrequency arrays to increase the statistical power of resting-state maps in monkeys. Neurolmage, 2018, 178, 287-294.	4.2	9
57	In vivo manganese tract tracing of frontal eye fields in rhesus macaques with ultra-high field MRI: Comparison with DWI tractography. NeuroImage, 2018, 181, 211-218.	4.2	12
58	Editorial Focus on "Invariant and heritable local cortical organization as revealed by fMRI― Journal of Neurophysiology, 2018, 120, 758-759.	1.8	0
59	Morphology-Specific Discrimination between MS White Matter Lesions and Benign White Matter Hyperintensities Using Ultra-High-Field MRI. American Journal of Neuroradiology, 2018, 39, 1473-1479.	2.4	21
60	Exogenous Neural Precursor Cell Transplantation Results in Structural and Functional Recovery in a Hypoxic-Ischemic Hemiplegic Mouse Model. ENeuro, 2018, 5, ENEURO.0369-18.2018.	1.9	20
61	Frontoparietal Functional Connectivity in the Common Marmoset. Cerebral Cortex, 2017, 27, 3890-3905.	2.9	78
62	Susceptibilityâ€weighted imaging using interâ€echoâ€variance channel combination for improved contrast at 7 tesla. Journal of Magnetic Resonance Imaging, 2017, 45, 1113-1124.	3.4	4
63	A geometrically adjustable receive array for imaging marmoset cohorts. NeuroImage, 2017, 156, 78-86.	4.2	14
64	Diffusion-weighted tractography in the common marmoset monkey at 9.4T. Journal of Neurophysiology, 2017, 118, 1344-1354.	1.8	25
65	Swallowing Preparation and Execution: Insights from a Delayed-Response Functional Magnetic Resonance Imaging (fMRI) Study. Dysphagia, 2017, 32, 526-541.	1.8	25
66	Initial Investigation into Microbleeds and White Matter Signal Changes following Radiotherapy for Low-Grade and Benign Brain Tumors Using Ultra-High-Field MRI Techniques. American Journal of Neuroradiology, 2017, 38, 2251-2256.	2.4	13
67	Reliable RF B/E-Field Probes for Time-Domain Monitoring of EM Exposure During Medical Device Testing. IEEE Transactions on Antennas and Propagation, 2017, 65, 4815-4823.	5.1	18
68	Multiparametric MRI changes persist beyond recovery in concussed adolescent hockey players. Neurology, 2017, 89, 2157-2166.	1.1	83
69	Spontaneous low frequency BOLD signal variations from resting-state fMRI are decreased in Alzheimer disease. PLoS ONE, 2017, 12, e0178529.	2.5	19
70	Medial Prefrontal and Anterior Insular Connectivity in Early Schizophrenia and Major Depressive Disorder: A Resting Functional MRI Evaluation of Large-Scale Brain Network Models. Frontiers in Human Neuroscience, 2016, 10, 132.	2.0	43
71	General Coupling Matrix Synthesis Pub _newline ? for Decoupling MRI RF Arrays. IEEE Transactions on Medical Imaging, 2016, 35, 2229-2242.	8.9	7
72	Metabolomics profiling of concussion in adolescent male hockey players: a novel diagnostic method. Metabolomics, 2016, 12, 1.	3.0	43

#	Article	IF	CITATIONS
73	Optimized parallel transmit and receive radiofrequency coil for ultrahigh-field MRI of monkeys. NeuroImage, 2016, 125, 153-161.	4.2	39
74	The Evaluation of Magnesium Chloride within a Polyethylene Glycol Formulation in a Porcine Model of Acute Spinal Cord Injury. Journal of Neurotrauma, 2016, 33, 2202-2216.	3.4	21
75	Neuroplastic Sensorimotor Resting State Network Reorganization in Children With Hemiplegic Cerebral Palsy Treated With Constraint-Induced Movement Therapy. Journal of Child Neurology, 2016, 31, 220-226.	1.4	27
76	Interâ€echo variance as a weighting factor for multiâ€channel combination in multiâ€echo acquisition for local frequency shift mapping. Magnetic Resonance in Medicine, 2015, 73, 1654-1661.	3.0	6
77	High Rate of Microbleed Formation following Primary Intracerebral Hemorrhage. International Journal of Stroke, 2015, 10, 1187-1191.	5.9	7
78	Design of a Parallel Transmit Head Coil at 7T With Magnetic Wall Distributed Filters. IEEE Transactions on Medical Imaging, 2015, 34, 836-845.	8.9	31
79	Resting State and Diffusion Neuroimaging Predictors of Clinical Improvements Following Constraint-Induced Movement Therapy in Children With Hemiplegic Cerebral Palsy. Journal of Child Neurology, 2015, 30, 1507-1514.	1.4	26
80	MRI RF Array Decoupling Method With Magnetic Wall Distributed Filters. IEEE Transactions on Medical Imaging, 2015, 34, 825-835.	8.9	28
81	Electrophysiological signatures of spontaneous BOLD fluctuations in macaque prefrontal cortex. NeuroImage, 2015, 113, 257-267.	4.2	38
82	Functional Imaging of Auditory Cortex in Adult Cats using High-field fMRI. Journal of Visualized Experiments, 2014, , e50872.	0.3	2
83	Origins of <i>R</i> ₂ ^{â^—} orientation dependence in gray and white matter. Proceedings of the National Academy of Sciences of the United States of America, 2014, 111, E159-67.	7.1	54
84	Highcor: A novel data-driven regressor identification method for BOLD fMRI. NeuroImage, 2014, 98, 184-194.	4.2	11
85	Multiple Sclerosis: Improved Identification of Disease-relevant Changes in Gray and White Matter by Using Susceptibility-based MR Imaging. Radiology, 2014, 272, 851-864.	7.3	50
86	Comparison of Multiecho Postprocessing Schemes for SWI with Use of Linear and Nonlinear Mask Functions. American Journal of Neuroradiology, 2014, 35, 38-44.	2.4	11
87	Increased deep gray matter iron is present in clinically isolated syndromes. Multiple Sclerosis and Related Disorders, 2014, 3, 194-202.	2.0	19
88	There's more than one way to scan a cat: Imaging cat auditory cortex with high-field fMRI using continuous or sparse sampling. Journal of Neuroscience Methods, 2014, 224, 96-106.	2.5	25
89	Identification of Optimal Structural Connectivity Using Functional Connectivity and Neural Modeling. Journal of Neuroscience, 2014, 34, 7910-7916.	3.6	138
90	Phase based venous suppression in resting-state BOLD GE-fMRI. NeuroImage, 2014, 100, 51-59.	4.2	25

#	Article	IF	CITATIONS
91	Isoflurane induces dose-dependent alterations in the cortical connectivity profiles and dynamic properties of the brain's functional architecture. Human Brain Mapping, 2014, 35, 5754-5775.	3.6	122
92	Resting-state networks show dynamic functional connectivity in awake humans and anesthetized macaques. Human Brain Mapping, 2013, 34, 2154-2177.	3.6	667
93	Reply. Annals of Neurology, 2013, 73, 797-797.	5.3	0
94	Characterization of the blood-oxygen level-dependent (BOLD) response in cat auditory cortex using high-field fMRI. NeuroImage, 2013, 64, 458-465.	4.2	25
95	Venocentric Lesions: An MRI Marker of MS?. Frontiers in Neurology, 2013, 4, 98.	2.4	13
96	Analysis of circumferential shielding as a methodto decouple radiofrequency coils for highâ€field MRI. Concepts in Magnetic Resonance Part B, 2013, 43B, 11-21.	0.7	5
97	A lowâ€cost, mechanically simple apparatus for measuring eddy currentâ€induced magnetic fields in MRI. NMR in Biomedicine, 2013, 26, 1285-1290.	2.8	2
98	Simultaneous in vivo pH and temperature mapping using a PARACESTâ€MRI contrast agent. Magnetic Resonance in Medicine, 2013, 70, 1016-1025.	3.0	66
99	Functional connectivity patterns of medial and lateral macaque frontal eye fields reveal distinct visuomotor networks. Journal of Neurophysiology, 2013, 109, 2560-2570.	1.8	30
100	Functional connectivity of the frontal eye fields in humans and macaque monkeys investigated with resting-state fMRI. Journal of Neurophysiology, 2012, 107, 2463-2474.	1.8	112
101	Poor Long-Term Blood Pressure Control After Intracerebral Hemorrhage. Stroke, 2012, 43, 2580-2585.	2.0	27
102	Mental chronometry. Neurolmage, 2012, 62, 1068-1071.	4.2	12
103	Information Processing Architecture of Functionally Defined Clusters in the Macaque Cortex. Journal of Neuroscience, 2012, 32, 17465-17476.	3.6	106
104	The great brain versus vein debate. NeuroImage, 2012, 62, 970-974.	4.2	43
105	Resting-State Connectivity Identifies Distinct Functional Networks in Macaque Cingulate Cortex. Cerebral Cortex, 2012, 22, 1294-1308.	2.9	61
106	A conformal transceive array for 7 T neuroimaging. Magnetic Resonance in Medicine, 2012, 67, 1487-1496.	3.0	51
107	Sliceâ€byâ€slice <i>B</i> ₁ ⁺ shimming at 7 T. Magnetic Resonance in Medicine, 2012, 68, 1109-1116.	3.0	58
108	Progressive membrane phospholipid changes in first episode schizophrenia with high field magnetic resonance spectroscopy. Psychiatry Research - Neuroimaging, 2012, 201, 25-33.	1.8	18

#	Article	IF	CITATIONS
109	Predictors of highly prevalent brain ischemia in intracerebral hemorrhage. Annals of Neurology, 2012, 71, 199-205.	5.3	119
110	Resting-state networks in the macaque at 7T. NeuroImage, 2011, 56, 1546-1555.	4.2	131
111	A radiofrequency coil to facilitate <i>B</i> shimming and parallel imaging acceleration in three dimensions at 7 T. NMR in Biomedicine, 2011, 24, 815-823.	2.8	41
112	A Canadian Perspective on Ethics Review and Neuroimaging: Tensions and Solutions. Canadian Journal of Neurological Sciences, 2011, 38, 572-579.	0.5	5
113	Grey matter and social functioning correlates of glutamatergic metabolite loss in schizophrenia. British Journal of Psychiatry, 2011, 198, 448-456.	2.8	103
114	In vivo detection of MRIâ€₽ARACEST agents in mouse brain tumors at 9.4 T. Magnetic Resonance in Medicine, 2011, 66, 67-72.	3.0	30
115	Elimination of the Vesicular Acetylcholine Transporter in the Striatum Reveals Regulation of Behaviour by Cholinergic-Glutamatergic Co-Transmission. PLoS Biology, 2011, 9, e1001194.	5.6	80
116	Evaluation of preprocessing steps to compensate for magnetic field distortions due to body movements in BOLD fMRI. Magnetic Resonance Imaging, 2010, 28, 235-244.	1.8	31
117	In vivo detection of PARACEST agents with relaxation correction. Magnetic Resonance in Medicine, 2010, 63, 1184-1192.	3.0	20
118	Transmit/receive radiofrequency coil with individually shielded elements. Magnetic Resonance in Medicine, 2010, 64, 1640-1651.	3.0	29
119	A cradle-shaped gradient coil to expand the clear-bore width of an animal MRI scanner. Physics in Medicine and Biology, 2010, 55, 497-514.	3.0	4
120	Visually-guided grasping produces fMRI activation in dorsal but not ventral stream brain areas. Journal of Vision, 2010, 1, 194-194.	0.3	2
121	Scene classification and parahippocampal place area activation in an individual with visual form agnosia. Journal of Vision, 2010, 2, 495-495.	0.3	3
122	Areas active during a pointing but not a saccade delay are medial to saccade-and-pointing network. Journal of Vision, 2010, 1, 265-265.	0.3	0
123	Differing viewpoint effects in the ventral and dorsal visual streams revealed using fMRI. Journal of Vision, 2010, 2, 45-45.	0.3	0
124	Visual and haptic object priming have a similar effect on fMRI activation in extra-striate cortex james@cerco.ups-tlse.fr. Journal of Vision, 2010, 1, 483-483.	0.3	0
125	Afterimages and pursuit: refining Helmholtz's theory of visual motion perception. Journal of Vision, 2010, 3, 602-602.	0.3	0
126	Neuroimaging Demonstration of Evolving Small Vessel Ischemic Injury in Cerebral Amyloid Angiopathy. Stroke, 2009, 40, e675-7.	2.0	32

#	Article	IF	CITATIONS
127	Longitudinal 4.0ÂTesla 31P magnetic resonance spectroscopy changes in the anterior cingulate and left thalamus in first episode schizophrenia. Psychiatry Research - Neuroimaging, 2009, 173, 155-157.	1.8	17
128	Optimized MRI contrast for onâ€resonance proton exchange processes of PARACEST agents in biological systems. Magnetic Resonance in Medicine, 2009, 62, 1282-1291.	3.0	7
129	BOLD fMRI activation for anti-saccades in nonhuman primates. NeuroImage, 2009, 45, 470-476.	4.2	50
130	A sensitive PARACEST contrast agent for temperature MRI: Eu ³⁺ â€DOTAMâ€glycine (Gly)â€phenylalanine (Phe). Magnetic Resonance in Medicine, 2008, 59, 374-381.	3.0	106
131	Functional MRI of oropharyngeal air-pulse stimulation. Neuroscience, 2008, 153, 1300-1308.	2.3	79
132	Hybrid two-dimensional navigator correction: A new technique to suppress respiratory-induced physiological noise in multi-shot echo-planar functional MRI. NeuroImage, 2008, 39, 1142-1150.	4.2	21
133	Connectivity of the Primate Superior Colliculus Mapped by Concurrent Microstimulation and Event-Related fMRI. PLoS ONE, 2008, 3, e3928.	2.5	30
134	Forebrain regions associated with postexercise differences in autonomic and cardiovascular function during baroreceptor unloading. American Journal of Physiology - Heart and Circulatory Physiology, 2007, 293, H299-H306.	3.2	25
135	Forebrain neural patterns associated with sex differences in autonomic and cardiovascular function during baroreceptor unloading. American Journal of Physiology - Regulatory Integrative and Comparative Physiology, 2007, 292, R715-R722.	1.8	46
136	Longitudinal grey-matter and glutamatergic losses in first-episode schizophrenia. British Journal of Psychiatry, 2007, 191, 325-334.	2.8	176
137	Sex differences in forebrain and cardiovagal responses at the onset of isometric handgrip exercise: a retrospective fMRI study. Journal of Applied Physiology, 2007, 103, 1402-1411.	2.5	62
138	Ventral medial prefrontal cortex and cardiovagal control in conscious humans. NeuroImage, 2007, 35, 698-708.	4.2	194
139	NMR Simulation Analysis of Statistical Effects on Quantifying Cerebrovascular Parameters. Biophysical Journal, 2007, 92, 1014-1021.	0.5	17
140	Perirhinal and hippocampal contributions to visual recognition memory can be distinguished from those of occipitoâ€ŧemporal structures based on conscious awareness of prior occurrence. Hippocampus, 2007, 17, 1081-1092.	1.9	38
141	Transceive surface coil array for MRI of the human prostate at 4T. Magnetic Resonance in Medicine, 2007, 57, 455-458.	3.0	14
142	Theoretical and Experimental Optimization of Laser Speckle Contrast Imaging for High Specificity to Brain Microcirculation. Journal of Cerebral Blood Flow and Metabolism, 2007, 27, 258-269.	4.3	105
143	EEG Monitoring during Functional MRI in Animal Models. Epilepsia, 2007, 48, 37-46.	5.1	28
144	Linear aspects of transformation from interictal epileptic discharges to BOLD fMRI signals in an an an animal model of occipital epilepsy. NeuroImage, 2006, 30, 1133-1148.	4.2	30

#	Article	IF	CITATIONS
145	Robust prescan calibration for multiple spin-echo sequences: application to FSE and b-SSFP. Magnetic Resonance Imaging, 2006, 24, 857-867.	1.8	12
146	Cerebral cortical processing of swallowing in older adults. Experimental Brain Research, 2006, 176, 12-22.	1.5	109
147	Grey and white matter differences in brain energy metabolism in first episode schizophrenia: 31P-MRS chemical shift imaging at 4 Tesla. Psychiatry Research - Neuroimaging, 2006, 146, 127-135.	1.8	50
148	Relaxometry model of strong dipolar perturbers for balanced-SSFP: Application to quantification of SPIO loaded cells. Magnetic Resonance in Medicine, 2006, 55, 583-591.	3.0	19
149	SENSE optimization of a transceive surface coil array for MRI at 4 T. Magnetic Resonance in Medicine, 2006, 56, 630-636.	3.0	10
150	Representation of Head-Centric Flow in the Human Motion Complex. Journal of Neuroscience, 2006, 26, 5616-5627.	3.6	44
151	Physiological monitoring of small animals during magnetic resonance imaging. Journal of Neuroscience Methods, 2005, 144, 207-213.	2.5	18
152	Cortical regions associated with autonomic cardiovascular regulation during lower body negative pressure in humans. Journal of Physiology, 2005, 569, 331-345.	2.9	185
153	Learning-related fMRI activation associated with a rotational visuo-motor transformation. Cognitive Brain Research, 2005, 22, 373-383.	3.0	93
154	Novelty responses to relational and non-relational information in the hippocampus and the parahippocampal region: A comparison based on event-related fMRI. Hippocampus, 2005, 15, 763-774.	1.9	149
155	Implementation issues of multivoxel STEAM-localized1H spectroscopy. Magnetic Resonance in Medicine, 2005, 53, 713-718.	3.0	12
156	Real-time display of artifact-free electroencephalography during functional magnetic resonance imaging and magnetic resonance spectroscopy in an animal model of epilepsy. Magnetic Resonance in Medicine, 2005, 53, 456-464.	3.0	27
157	Transceive surface coil array for magnetic resonance imaging of the human brain at 4 T. Magnetic Resonance in Medicine, 2005, 54, 499-503.	3.0	45
158	Modeling and suppression of respiration-related physiological noise in echo-planar functional magnetic resonance imaging using global and one-dimensional navigator echo correction. Magnetic Resonance in Medicine, 2005, 54, 411-418.	3.0	29
159	Discrete functional contributions of cerebral cortical foci in voluntary swallowing: a functional magnetic resonance imaging (fMRI) ?Go, No-Go? study. Experimental Brain Research, 2005, 161, 81-90.	1.5	84
160	Functional connectivity of dissociative responses in posttraumatic stress disorder: A functional magnetic resonance imaging investigation. Biological Psychiatry, 2005, 57, 873-884.	1.3	238
161	A 4.0-T fMRI study of brain connectivity during word fluency in first-episode schizophrenia. Schizophrenia Research, 2005, 75, 247-263.	2.0	124
162	The Nature of Traumatic Memories: A 4-T fMRI Functional Connectivity Analysis. American Journal of Psychiatry, 2004, 161, 36-44.	7.2	224

#	Article	IF	CITATIONS
163	Behavioral and Neuroimaging Evidence for a Contribution of Color and Texture Information to Scene Classification in a Patient with Visual Form Agnosia. Journal of Cognitive Neuroscience, 2004, 16, 955-965.	2.3	80
164	Focal changes in brain energy and phospholipid metabolism in first-episode schizophrenia. British Journal of Psychiatry, 2004, 184, 409-415.	2.8	51
165	Spared somatomotor and cognitive functions in a patient with a large porencephalic cyst revealed by fMRI. Neuropsychologia, 2004, 42, 405-418.	1.6	9
166	Duration of untreated psychosis vs. N-acetylaspartate and choline in first episode schizophrenia: a 1H magnetic resonance spectroscopy study at 4.0 Tesla. Psychiatry Research - Neuroimaging, 2004, 131, 107-114.	1.8	46
167	Comparative study of proton and phosphorus magnetic resonance spectroscopy in schizophrenia at 4 Tesla. Psychiatry Research - Neuroimaging, 2004, 132, 33-39.	1.8	21
168	Noise properties of a NMR transceiver coil array. Journal of Magnetic Resonance, 2004, 171, 151-156.	2.1	22
169	Sodium T2*-weighted MR imaging of acute focal cerebral ischemia in rabbits. Magnetic Resonance Imaging, 2004, 22, 983-991.	1.8	20
170	Human cardiovascular and gustatory brainstem sites observed by functional magnetic resonance imaging. Journal of Comparative Neurology, 2004, 471, 446-461.	1.6	62
171	Robust automated shimming technique using arbitrary mapping acquisition parameters (RASTAMAP). Magnetic Resonance in Medicine, 2004, 51, 881-887.	3.0	83
172	Long component time constant of23NaT*2 relaxation in healthy human brain. Magnetic Resonance in Medicine, 2004, 52, 407-410.	3.0	32
173	Cerebral Areas Processing Swallowing and Tongue Movement Are Overlapping but Distinct: A Functional Magnetic Resonance Imaging Study. Journal of Neurophysiology, 2004, 92, 2428-2443.	1.8	252
174	Comparison of Memory- and Visually Guided Saccades Using Event-Related fMRI. Journal of Neurophysiology, 2004, 91, 873-889.	1.8	99
175	Visually guided grasping produces fMRI activation in dorsal but not ventral stream brain areas. Experimental Brain Research, 2003, 153, 180-189.	1.5	636
176	An MRI study of subgenual prefrontal cortex in patients with familial and non-familial bipolar I disorder. Journal of Affective Disorders, 2003, 77, 167-171.	4.1	73
177	Recall of emotional states in posttraumatic stress disorder: an fMRI investigation. Biological Psychiatry, 2003, 53, 204-210.	1.3	299
178	Transient hemodynamics during a breath hold challenge in a two part functional imaging study with simultaneous near-infrared spectroscopy in adult humans. NeuroImage, 2003, 20, 1246-1252.	4.2	59
179	Interaction of Retinal Image and Eye Velocity in Motion Perception. Neuron, 2003, 39, 569-576.	8.1	20
180	Individual Differences in a Husband and Wife Who Developed PTSD After a Motor Vehicle Accident: A Functional MRI Case Study. American Journal of Psychiatry, 2003, 160, 667-669.	7.2	73

#	Article	IF	CITATIONS
181	Flexible Retinotopy: Motion-Dependent Position Coding in the Visual Cortex. Science, 2003, 302, 878-881.	12.6	136
182	Glutamate and Glutamine in the Anterior Cingulate and Thalamus of Medicated Patients With Chronic Schizophrenia and Healthy Comparison Subjects Measured With 4.0-T Proton MRS. American Journal of Psychiatry, 2003, 160, 2231-2233.	7.2	254
183	Preparatory Set Associated With Pro-Saccades and Anti-Saccades in Humans Investigated With Event-Related fMRI. Journal of Neurophysiology, 2003, 89, 1016-1023.	1.8	234
184	Influence of hypoxia on wavelength dependence of differential pathlength and near-infrared quantification. Physics in Medicine and Biology, 2002, 47, 1573-1589.	3.0	10
185	Glutamate and Glutamine Measured With 4.0 T Proton MRS in Never-Treated Patients With Schizophrenia and Healthy Volunteers. American Journal of Psychiatry, 2002, 159, 1944-1946.	7.2	386
186	Imaging Attentional Modulation of Pain in the Periaqueductal Gray in Humans. Journal of Neuroscience, 2002, 22, 2748-2752.	3.6	527
187	Region-specific changes in phospholipid metabolism in chronic, medicated schizophrenia. British Journal of Psychiatry, 2002, 180, 39-44.	2.8	49
188	Brain activation during script-driven imagery induced dissociative responses in PTSD: a functional magnetic resonance imaging investigation. Biological Psychiatry, 2002, 52, 305-311.	1.3	470
189	High resolution fMRI of ocular dominance columns within the visual cortex of human amblyopes. Strabismus, 2002, 10, 129-136.	0.7	52
190	Noise Reduction in BOLD-Based fMRI Using Component Analysis. NeuroImage, 2002, 17, 1521-1537.	4.2	248
191	Differential Effects of Viewpoint on Object-Driven Activation in Dorsal and Ventral Streams. Neuron, 2002, 35, 793-801.	8.1	258
192	Haptic study of three-dimensional objects activates extrastriate visual areas. Neuropsychologia, 2002, 40, 1706-1714.	1.6	367
193	Postacquisition suppression of large-vessel BOLD signals in high-resolution fMRI. Magnetic Resonance in Medicine, 2002, 47, 1-9.	3.0	194
194	In vivo brain31P-MRS: measuring the phospholipid resonances at 4 Tesla from small voxels. NMR in Biomedicine, 2002, 15, 338-347.	2.8	64
195	Human fMRI evidence for the neural correlates of preparatory set. Nature Neuroscience, 2002, 5, 1345-1352.	14.8	319
196	Distinguishing Subregions of the Human MT+ Complex Using Visual Fields and Pursuit Eye Movements. Journal of Neurophysiology, 2001, 86, 1991-2000.	1.8	251
197	Cerebral Cortical Representation of Automatic and Volitional Swallowing in Humans. Journal of Neurophysiology, 2001, 85, 938-950.	1.8	345
198	Brief visual stimulation allows mapping of ocular dominance in visual cortex using fMRI. Human Brain Mapping, 2001, 14, 210-217.	3.6	139

#	Article	IF	CITATIONS
199	Imaging function in the working brain with fMRI. Current Opinion in Neurobiology, 2001, 11, 630-636.	4.2	38
200	Neural Correlates of Traumatic Memories in Posttraumatic Stress Disorder: A Functional MRI Investigation. American Journal of Psychiatry, 2001, 158, 1920-1922.	7.2	473
201	Spatial and temporal resolution in fMRI. , 2001, , 146-158.		5
202	A transmit-only/receive-only (TORO) RF system for high-field MRI/MRS applications. Magnetic Resonance in Medicine, 2000, 43, 284-289.	3.0	141
203	Comparison of the quantification precision of human short echo time1H spectroscopy at 1.5 and 4.0 Tesla. Magnetic Resonance in Medicine, 2000, 44, 185-192.	3.0	128
204	Spectroscopic lineshape correction by QUECC: Combined QUALITY deconvolution and eddy current correction. Magnetic Resonance in Medicine, 2000, 44, 641-645.	3.0	76
205	The effects of visual object priming on brain activation before and after recognition. Current Biology, 2000, 10, 1017-1024.	3.9	161
206	An fMRI study of the selective activation of human extrastriate form vision areas by radial and concentric gratings. Current Biology, 2000, 10, 1455-1458.	3.9	237
207	A Comparison of Frontoparietal fMRI Activation During Anti-Saccades and Anti-Pointing. Journal of Neurophysiology, 2000, 84, 1645-1655.	1.8	283
208	BOLD fMRI Response of Early Visual Areas to Perceived Contrast in Human Amblyopia. Journal of Neurophysiology, 2000, 84, 1907-1913.	1.8	98
209	The employment of the insane. British Journal of Psychiatry, 2000, 176, 401-401.	2.8	0
210	Eye Position Signal Modulates a Human Parietal Pointing Region during Memory-Guided Movements. Journal of Neuroscience, 2000, 20, 5835-5840.	3.6	120
211	Motor Area Activity During Mental Rotation Studied by Time-Resolved Single-Trial fMRI. Journal of Cognitive Neuroscience, 2000, 12, 310-320.	2.3	461
212	Recovery of fMRI Activation in Motion Area MT Following Storage of the Motion Aftereffect. Journal of Neurophysiology, 1999, 81, 388-393.	1.8	102
213	Perception of the Mccollough Effect Correlates with Activity in Extrastriate Cortex: A Functional Magnetic Resonance Imaging Study. Psychological Science, 1999, 10, 444-448.	3.3	22
214	Submillimeter functional localization in human striate cortex using BOLD contrast at 4 Tesla: Implications for the vascular point-spread function. Magnetic Resonance in Medicine, 1999, 41, 230-235.	3.0	155
215	Human forebrain activation by visceral stimuli. , 1999, 413, 572-582.		179
216	Dissociating Pain from Its Anticipation in the Human Brain. Science, 1999, 284, 1979-1981.	12.6	1,026

#	Article	IF	CITATIONS
217	Spatial and temporal limits in cognitive neuroimaging with fMRI. Trends in Cognitive Sciences, 1999, 3, 207-216.	7.8	182
218	fMRI evidence for an inverted face representation in human somatosensory cortex. NeuroReport, 1999, 10, 1393-1395.	1.2	45
219	Repetition priming and the time course of object recognition. NeuroReport, 1999, 10, 1019-1023.	1.2	39
220	Human forebrain activation by visceral stimuli. Journal of Comparative Neurology, 1999, 413, 572-582.	1.6	2
221	Reduced visual evoked responses in multiple sclerosis patients with optic neuritis: Comparison of functional magnetic resonance imaging and visual evoked potentials. Multiple Sclerosis Journal, 1999, 5, 161-164.	3.0	5
222	Amplitude response and stimulus presentation frequency response of human primary visual cortex using BOLD EPI at 4 T. Magnetic Resonance in Medicine, 1998, 40, 203-209.	3.0	72
223	Spatial and temporal resolution of functional magnetic resonance imaging. Biochemistry and Cell Biology, 1998, 76, 560-571.	2.0	31
224	ON THE CHARACTERISTICS OF FUNCTIONAL MAGNETIC RESONANCE IMAGING OF THE BRAIN. Annual Review of Biophysics and Biomolecular Structure, 1998, 27, 447-474.	18.3	285
225	Effect of Luminance Contrast on BOLD fMRI Response in Human Primary Visual Areas. Journal of Neurophysiology, 1998, 79, 2204-2207.	1.8	78
226	Mental chronometry using latency-resolved functional MRI. Proceedings of the National Academy of Sciences of the United States of America, 1998, 95, 10902-10907.	7.1	228
227	Spatial and temporal resolution of functional magnetic resonance imaging. Biochemistry and Cell Biology, 1998, 76, 560-571.	2.0	19
228	Ocular Dominance in Human V1 Demonstrated by Functional Magnetic Resonance Imaging. Journal of Neurophysiology, 1997, 77, 2780-2787.	1.8	282
229	Differences in perceived shape from shading correlate with activity in early visual areas. Current Biology, 1997, 7, 144-147.	3.9	115
230	The functional scout image: Immediate mapping of cortical function at 4 tesla using receiver phase cycling. Magnetic Resonance in Medicine, 1997, 38, 183-186.	3.0	10
231	Experimental determination of the BOLD field strength dependence in vessels and tissue. Magnetic Resonance in Medicine, 1997, 38, 296-302.	3.0	474
232	Investigation of BOLD contrast in fMRI using multi-shot EPI. NMR in Biomedicine, 1997, 10, 179-182.	2.8	50
233	31P magnetic resonance spectroscopy of the Sherpa heart: a phosphocreatine/adenosine triphosphate signature of metabolic defense against hypobaric hypoxia Proceedings of the National Academy of Sciences of the United States of America, 1996, 93, 1215-1220.	7.1	96
234	BOLD Based Functional MRI at 4 Tesla Includes a Capillary Bed Contribution: Echo-Planar Imaging Correlates with Previous Optical Imaging Using Intrinsic Signals. Magnetic Resonance in Medicine, 1995, 33, 453-459.	3.0	407

#	Article	IF	CITATIONS
235	High contrast and fast threeâ€dimensional magnetic resonance imaging at high fields. Magnetic Resonance in Medicine, 1995, 34, 308-312.	3.0	225
236	Comparison of T2*-weighted sequences for functional MRI. International Journal of Imaging Systems and Technology, 1995, 6, 184-190.	4.1	0
237	High-temporal-resolution studies of the human primary visual cortex at 4 T: Teasing out the oxygenation contribution in FMRI. International Journal of Imaging Systems and Technology, 1995, 6, 209-215.	4.1	14
238	Spectroscopic Imaging of Circular Voxels with a Two-Dimensional Fourier-Series Window Technique. Journal of Magnetic Resonance Series B, 1994, 105, 225-232.	1.6	25
239	Functional Imaging of the Brain by Nuclear Magnetic Resonance. , 1994, , 137-150.		6
240	4 Tesla gradient recalled echo characteristics of photic stimulation-induced signal changes in the human primary visual cortex. Magnetic Resonance in Medicine, 1993, 30, 380-386.	3.0	405
241	Functional brain mapping by blood oxygenation level-dependent contrast magnetic resonance imaging. A comparison of signal characteristics with a biophysical model. Biophysical Journal, 1993, 64, 803-812.	0.5	1,620
242	Functional imaging of human motor cortex at high magnetic field. Journal of Neurophysiology, 1993, 69, 297-302.	1.8	339
243	Intrinsic signal changes accompanying sensory stimulation: functional brain mapping with magnetic resonance imaging Proceedings of the National Academy of Sciences of the United States of America, 1992, 89, 5951-5955.	7.1	3,216
244	Functional Brain Mapping Using Magnetic Resonance Imaging: Signal Changes Accompanying Visual Stimulation. Investigative Radiology, 1992, 27, S47-S53.	6.2	97
245	31P NMR spectroscopy of the human heart at 4 T: Detection of substantially uncontaminated cardiac spectra and differentiation of subepicardium and subendocardium. Magnetic Resonance in Medicine, 1992, 26, 368-376.	3.0	61
246	Proton Relaxation Studies of Water Compartmentalization in a Model Neurological System. Magnetic Resonance in Medicine, 1992, 28, 264-274.	3.0	87
247	Multiexponential proton relaxation in model cellular systems. Magnetic Resonance in Medicine, 1991, 20, 196-213.	3.0	46
248	Application of continuous relaxation time distributions to the fitting of data from model systmes and excised tissue. Magnetic Resonance in Medicine, 1991, 20, 214-227.	3.0	130
249	Solvent proton relaxation of aqueous solutions of the serum proteins alpha 2-macroglobulin, fibrinogen, and albumin. Biophysical Journal, 1990, 57, 389-396.	0.5	22
250	Quantitative separation of NMR images of water in wood on the basis of T2. Journal of Magnetic Resonance, 1989, 82, 205-210.	0.5	18
251	An NMR determination of the physiological water distribution in wood during drying. Journal of Applied Polymer Science, 1987, 33, 1141-1155.	2.6	132